Sentinel-2 data classification for land use land cover mapping in northern Algeria

Nadia Zikiou, Holly Rushmeier

Nadia Zikiou, Holly Rushmeier, "Sentinel-2 data classification for land use land cover mapping in northern Algeria," Proc. SPIE 12519, Algorithms, Technologies, and Applications for Multispectral and Hyperspectral Imaging XXIX
, 125190H (13 June 2023); doi: 10.1117/12.2664856

SPIE.

Event: SPIE Defense + Commercial Sensing, 2023, Orlando, Florida, United States

Sentinel-2 Data Classification for Land Use Land Cover Mapping in Northern Algeria

Nadia Zikiou*[a], Holly Rushmeier[b]
[a]Yale Institute for Biospheric Studies, 170 Whitney Avenue, RM 213A, New Haven , CT, 65011, [b,a]Dept. of Computer Science, A.K. Watson Hall, 51 Prospect Street, New Haven, CT, 06511.

Abstract

The study of land use and land cover (LULC) changes is essential to understand the impact of human activities on the environment. The North of Algeria is a region that experiences high rates of change in LULC, making it a suitable study area. In this research, the potential of Sentinel-2 attributes for LULC classification in this region is evaluated using a deep learning-based approach. To improve the efficiency of the model, six reflectance-based indices are calculated to highlight the region of interest. The results are compared to the USGS land cover change data and show promising LULC change detection. In order to verify the presence of missed classes in our land use/land cover classification results, we employed a CNN-object detection method using high-resolution Planetscope images. This study demonstrates the potential of Sentinel-2 attributes for accurate LULC classification and change detection in the North of Algeria, which can be useful for monitoring land use patterns and planning sustainable land management practices.

Keywords: LULC classification, Sentinel-2 images, Conventional Neural Networks, Deep learning, ResNet50 model, Feature extraction, Planetscope images, Urban index, vegetation.

1. Introduction

The surface of our planet is in a constant state of flux, influenced by a variety of factors, including both natural events like wildfires and floods, and human activities such as manufacturing and urban development [1, 2]. Having precise data on land use land cover (LULC) can assist in multiple research undertakings concerning wildfires, floods, droughts, forest fragmentation, and climate change across different levels. To effectively manage resources, it is crucial to detect and monitor these changes [3]. One highly efficient method for monitoring such changes, especially over vast and inaccessible areas, is through the use of remote sensing (RS) technology. RS imagery allows for a wide coverage of areas at different points in time and is also cost- and time-effective [4, 5, 6]. Remote sensing applications involve analyzing and contrasting alterations between various remote sensing images and correlated data from different timeframes using mathematical models and image processing techniques. Change detection has become increasingly significant in recent times as it finds applications in land and resource management, monitoring of agricultural and forestry sectors, and assessment of natural disasters [7]. Additionally, by employing both visual and digital image processing techniques, it becomes feasible to extract crucial biophysical information from the vegetation cover. This information is essential in understanding various processes such as forest distribution, human activities, urban management, and biodiversity conservation. Numerous vegetation indices exist that are uniquely suitable to facilitate the acquisition of spectral response information from objects [8]. These indices allow the diagnosis of various

Algorithms, Technologies, and Applications for Multispectral and Hyperspectral Imaging XXIX,
edited by Miguel Velez-Reyes, David W. Messinger, Proc. of SPIE Vol. 12519,
125190H · © 2023 SPIE · 0277-786X · doi: 10.1117/12.2664856

biophysical parameters such as leaf area index, biomass, burn areas, land cover percentage, and productivity. In [5], the authors conducted research to assess the effectiveness of various vegetation indices such as NDVI [9, 10], SAVI [11], LAI [12], EVI [13], and NDWI [14] in the classification of land use and cover. The objective was to identify the index that closely resembled the classification carried out by the MaxVer algorithm and best represented the coverage. The study revealed that no single vegetation index performed well across all the evaluated classes. However, NDVI, EVI, and SAVI showed good adjustments in most of the thematic classes. Based on their findings, the authors concluded that the choice of the most suitable vegetation index for land use and land cover classification depends mainly on the predominant soil use.

The NBR+ index, which is a modified version of the Normalized Burn Ratio (NBR) index, was found to be more efficient than both the NBR and the Burned Area Index (BAI) in a study conducted by the authors in [15]. The NBR+ index was proposed to address some of the limitations of the NBR index, which is commonly used to assess fire severity and vegetation recovery following wildfires. The NBR index uses the difference between near-infrared and shortwave infrared reflectance to identify changes in vegetation cover and the extent of burned areas. However, it can also be affected by other factors, such as topography and atmospheric conditions, which can reduce its accuracy. In contrast, the NBR+ index incorporates a correction factor that accounts for differences in topography and atmospheric conditions, making it more robust and accurate than the NBR index. The authors in [15] conducted a study comparing the performance of the NBR+, NBR, and BAI indices in assessing post-fire vegetation recovery, and found that the NBR+ index was more efficient and accurate than the other two indices. Therefore, based on the findings of this study, the NBR+ index may be a better choice for assessing fire severity and vegetation recovery following wildfires.

Land use and land cover mapping using spectral indices can provide valuable information about the distribution and characteristics of different land cover types. However, it is important to note that spectral indices alone may not provide a complete picture of the land cover types and may have some limitations.

Over the past years, several studies have concentrated on land use land cover (LULC) classification by employing machine learning techniques on various remote sensing data. Due to the effectiveness of machine learning (ML) in several applications of GIS and remote sensing, support vector machine (SVM) [16, 17, 18] and random forest (RF) [19] statistical methods are frequently employed in LULC mapping [20]. These methods have been integrated into GIScience software packages. As a subset of machine learning (ML), Deep Learning (DL) has the capability to execute artificial intelligence tasks through extensive training resources. Different deep-learning techniques have been proposed for LULC in remote sensing (RS) imagery. These techniques include convolutional neural networks (CNN)[21], deep belief networks (DBNs)[22], recurrent neural networks (RNN), and auto-encoder (AE)[23].

This study aims to Map land use and land cover change in northern Algeria for the period between 2016 and 2022. This will provide important information about the changes in land cover types and the drivers of these changes. This information can be used to inform land management policies and conservation efforts, as well as to monitor the impact of human activities on the environment. Within this region, there exists a wide range of plant and animal species that are crucial for maintaining the resilience of the ecosystem. However, the area is currently facing a threat to its biodiversity due to land use changes such as habitat loss, overexploitation of resources, and the impact of climate change. Spectral indices such as the Normalized Difference Vegetation Index (NDVI), Normalized Burn Ratio (NBR), and Normalized Difference Built-up Index (NDBI) are used to distinguish between different land cover types, such as natural forests, water bodies, and urban areas. These indices are then used to highlight accurately the Regions of interest (ROI) that we have used as inputs for the CNN tool. The results are compared to the USGS dataset.

The manuscript is divided into five main sections, each of which is dedicated to a specific topic related to the study. Section 2 provides a thorough description of the study area and the materials used. Section 3 provides an explanation of the methodology. Section 4 presents the results of the study and provides a discussion of these findings. Finally, the manuscript concludes with a final section that summarizes the main points and conclusions of the study.

2. Data and materials

2.1. Study area

Tizi Ouzou and Bejaia are two cities located in the northern region of Algeria. Tizi Ouzou is situated in the heart of the Djurdjura mountain range, while Bejaia is located on the coast of the Mediterranean Sea. The geography of Tizi Ouzou is characterized by its mountainous terrain, with peaks rising to over 2,000 meters above sea level. Bejaia, on the other hand, has a relatively flat coastal plain, with rugged hills and mountains in the surrounding area. In terms of climate, Tizi Ouzou experiences a continental climate with hot summers and cold winters, while Bejaia has a Mediterranean climate with mild winters and warm summers. Both cities receive a significant amount of rainfall throughout the year, with the wettest months being from October to March.

These two cities are highly susceptible to fires every year. In 2021, the fire incidents in these regions reached an alarming rate, posing a significant threat to the local flora and fauna, as well as the inhabitants. According to the National Office of Meteorology (https://www.aps.dz/en/algeria/tag/National%20Meteorological%20Office), the forests and mountainous areas of Tizi Ouzou were hit by more than 120 fires, while Bejaia experienced over 70 wildfires. These devastating events are due to a combination of factors, including high temperatures, strong winds, and the lack of necessary equipment to combat these fires.

Apart from the frequent fire outbreaks, the humid climate during the winters in these regions has led to serious erosion problems. The National Agency for Soil Conservation reported that approximately 40% of the land in the northern region of Algeria is exposed to erosion due to a lack of vegetation cover, deforestation, and human activities [24]. The heavy rainfall during the winter season exacerbates the erosion problem, leading to a loss of soil fertility and a reduction in agricultural productivity. Therefore, measures need to be taken to prevent fires and erosion in these regions to protect the environment and the livelihoods of the local communities.

The regions have also been affected by land-use change due to settlement and human activities. According to the National Office of Statistics, the urbanized area of Tizi Ouzou increased by 68% between 1987 and 2008, while Bejaia's urbanized area expanded by 83% during the same period. The United Nations World Urbanization Prospects (https://population.un.org/wup/Country-Profiles/) reported that the level of urbanization in Algeria increased from 73.1% in 2016 to 74.7% in 2020. The increase in urbanization has led to the conversion of agricultural land and forest areas into built-up areas, resulting in a loss of biodiversity and ecosystem services.

In addition to urbanization, agricultural activities, and grazing have also contributed to land-use change in these regions. The National Institute of Agronomic Research (https://www.era-learn.eu/network-information/organisations/institut-national-de-la-recherche-agronomique) reported that agricultural land in Tizi Ouzou and Bejaia decreased by 15% between 2000 and 2016, with a significant increase in grazing land. According to the FAOSTAT database (https://www.fao.org/faostat/en/#data), which provides statistics on food and agriculture, the percentage of agricultural land in Algeria decreased from 17.97% in 2016 to 17.58% in 2020. The overuse of grazing land has led to the degradation of soil quality and the loss of vegetation cover, exacerbating the erosion problem.

Overall, settlement and human activities have led to significant land-use change in Tizi Ouzou and Bejaia, with the conversion of forest and agricultural land into built-up areas and grazing land. These activities have contributed to the erosion problem, as well as the loss of biodiversity and ecosystem services, highlighting the need for sustainable land-use practices in these regions.

Our study area is located between 36°26'22" N to 36°55'11" N and 4°7'43" E to 5°9'11" E and encompasses an area of 371,838 hectares (ha) (See Figure 1). This region is characterized by a diverse range of plant and animal species that support the overall health and stability of the ecosystem. Some of the notable species found in the area include the Atlas Cedar, Algerian iris, Barbary macaque, Barbary ground squirrel, and African wild dog. However, the region is also facing land change affecting its biodiversity, including habitat loss, overexploitation of resources, and climate change.

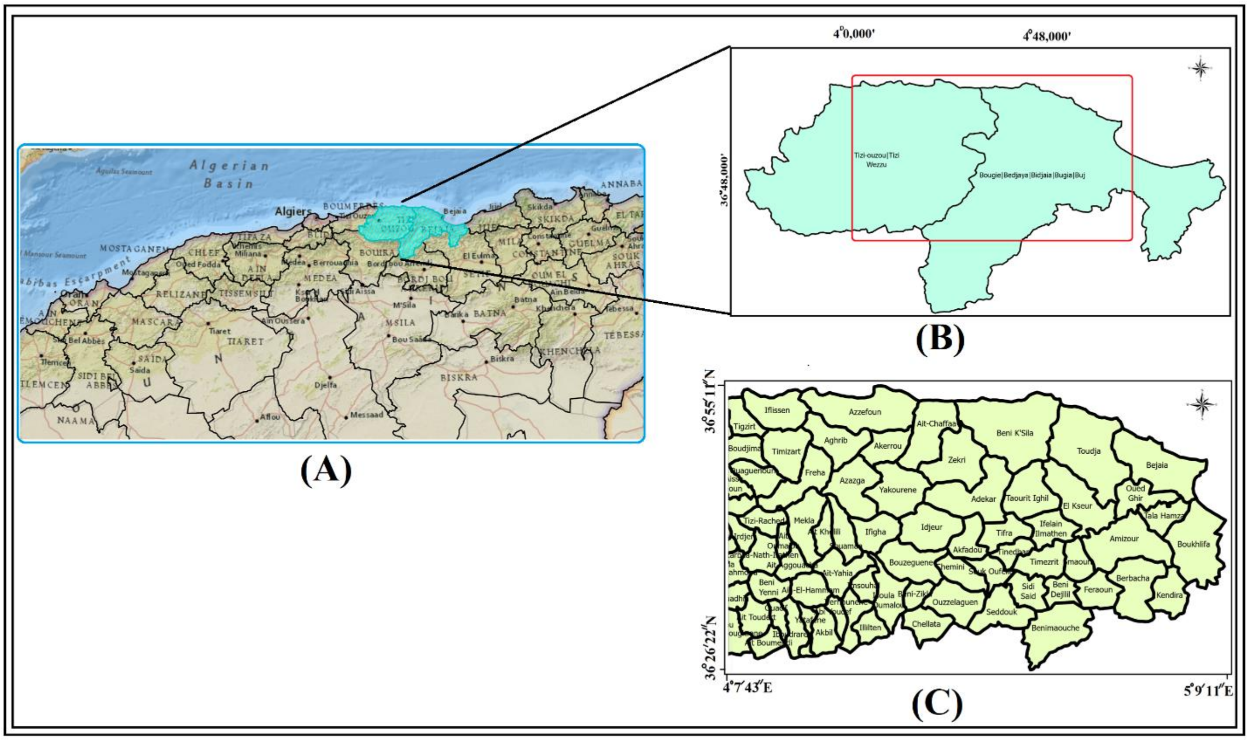

Figure I. The study area. **(A)** Location of the study area in northern Algeria, **(B)** Administrative Cities *Béjaïa* and Tizi Ouzou, **(C)** The selected study area.

2.2. Materials

2.2.1. Sentinel 2

Sentinel-2 images are an interesting tool for remote sensing applications, such as monitoring vegetation, detecting changes in land use, and assessing the health of natural resources. The images are captured by the Sentinel-2 satellite, which is equipped with a high-resolution multispectral imaging instrument that can observe the Earth's surface in 13 spectral bands. Sentinel-2 images provide a wealth of information that can be used to understand the dynamics of the Earth's surface, including its vegetation, water bodies, and urban areas. These images are freely available to the public (https://scihub.copernicus.eu), making them accessible to researchers and practitioners around the world.

To analyze the Land Cover Land Use changes over our study area, we have downloaded Sentinel-2 Level-1C images for the years 2016 through 2022, which were all captured in October of each year. These data provide a comprehensive view of the Earth's surface during that specific period. By examining the images, we can observe any changes or patterns that have occurred over time, such as changes in land use, vegetation growth, or water bodies.

2.2.2. Planet

Planetscope is a satellite-based imaging system that provides high-resolution images of the Earth's surface. These images are captured by a constellation of small satellites that are designed to deliver frequent revisits to any location on the planet. The Planetscope system is known for its high spatial resolution of 3 meters, which allows for detailed observation of the Earth's surface. This level of detail makes Planetscope imagery useful for a wide range of applications, such as monitoring land use, tracking urban growth, and assessing the impact of natural disasters. With its ability to provide up-to-date and high-quality images, Planetscope has become an essential tool for remote sensing and Earth observation.

While Planetscope images lack a Short-Wave Infrared (SWIR) band, which can make it challenging to calculate some spectral indices such as NDBI or NBR+, they offer a high spatial resolution that can be valuable for certain applications. In our study, we aim to leverage the high resolution of Planetscope images to detect areas that may not be easily discernible in Sentinel-2 images. By carefully examining the imagery, we can look for subtle changes or patterns that may be missed in lower-resolution images. While some limitations exist, such as the lack of a SWIR band, we can still extract useful information from Planetscope imagery. Ultimately, by combining the strengths of both Sentinel-2 and Planetscope data, we can obtain a more complete and accurate understanding of the LULC changes in our study area.

2.2.3. Comparison with the USGS

USGS Earth Explorer is a web-based tool that allows users to search, download, and process satellite imagery and other geospatial data (https://earthexplorer.usgs.gov). One of the primary applications of Earth Explorer is land cover detection, which involves using satellite imagery to identify and classify different types of land cover, such as forests, urban areas, and water bodies. With Earth Explorer, users can access a vast array of satellite images and data from various sources, which can be used to detect changes in land cover over time. By comparing images captured at different times, it is possible to track changes in land cover, such as deforestation, urbanization, or natural disasters. This information can be valuable for a wide range of applications, including environmental monitoring, land management, and disaster response planning. USGS Earth Explorer is an essential tool for researchers who need access to accurate and up-to-date information about the Earth's surface.

To analyze land cover changes over time in our study area and compare the Sentinel 2 results, we have downloaded the MCD12Q1 V6 dataset from the MODIS Land Cover- V6 collection in NAZA LPDAAC. This dataset contains information on land cover types in the selected region. Specifically, we have obtained data for the years 2016 to 2020, which allowed us to track changes in land cover over this period. The data for the years 2021 and 2022 are currently unavailable, which limited our ability to track more recent changes.

3. Methodology

3.1. Principle

The methodology employed in this study involves a multi-step process for verifying land cover in the study area. The first step involves the use of the Sentinel 2 detected images and six spectral indices to create the regions of interest for the deep learning model. The decision to use these indices was based on the nature of the study area, which includes multiple land cover classes, including overlapped areas. The spectral indices provide additional information that can help to highlight the Region of Interest (RoI) more efficiently in the study area, allowing more accurate classification of land cover. The use of spectral indices is especially important when dealing with complex land cover scenarios, as they can improve the effectiveness and robustness of the deep learning model. This allows for an accurate and targeted approach to training the model. Before the training process, the classification or detection models are chosen based on the research objectives. The data is then exported, and a training process is executed based on the exported data model and the selected parameters (Model type, Batch size, Validation percentage). The resulting model definition is used to classify the input rasters with the deep learning tool. Finally, changes between the raster images of 2016 and 2022 are detected using this approach. The approach process is shown in Figure 2.

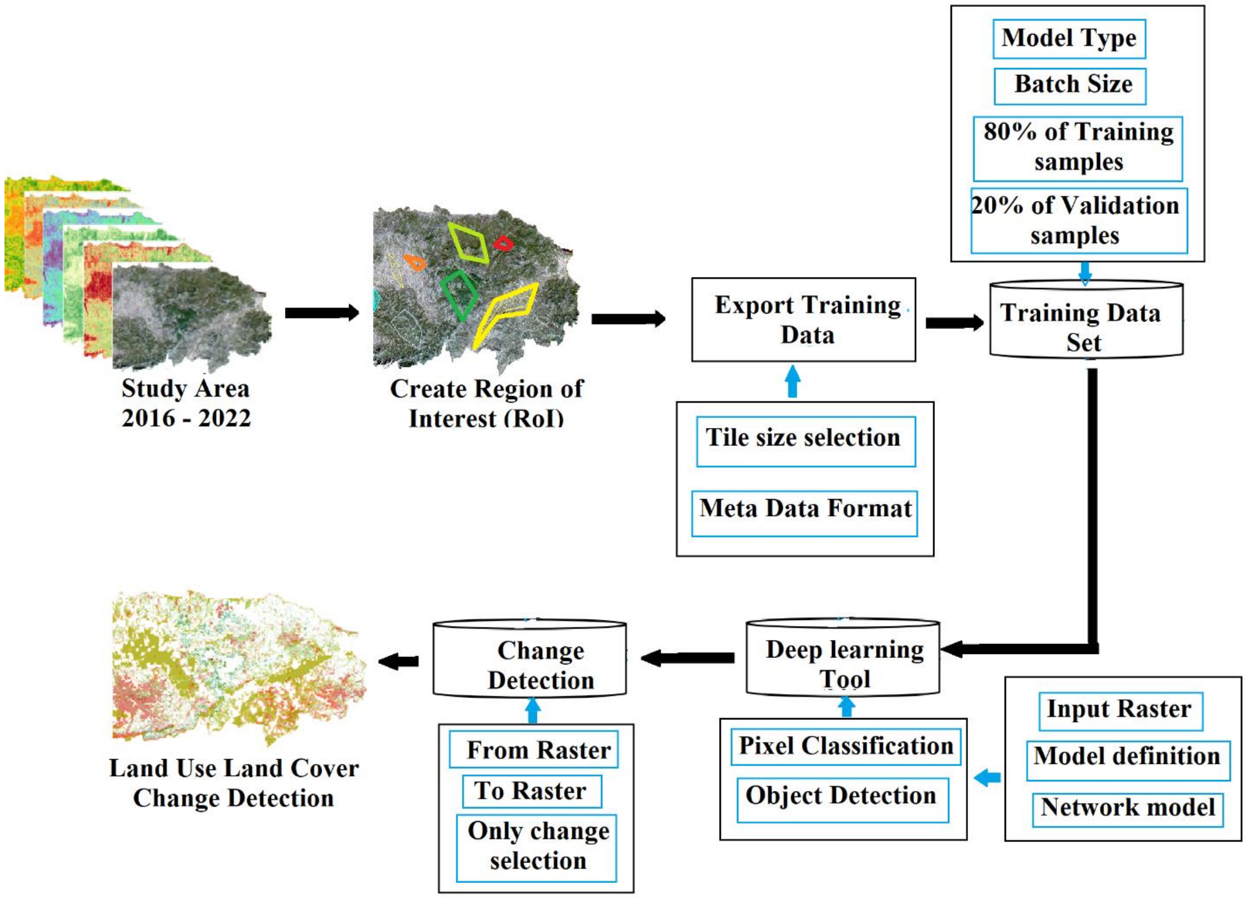

Figure 2. Principle of the CNN-based Land Change Detection approach.

In this study, the selection of seven land cover classes was based on prior knowledge of the study area allowing the identification of the most relevant and representative land cover classes that are likely to be present in the study area. A description of these classes is given in Table 1.

Table 1. Description of the classes

LULC types	Description
Land bare	Areas of land that are degraded because of fire, erosion, or human uses
Grassland	Areas dominated by grass
Settlement	Areas with build-up and rural parts are typically characterized by the presence of buildings and human habitation. These areas can range from small to big villages with a population that exceeds 50,000
Woodland	Forested areas with a mix of trees (such as cork oak and the zéen oak) and open spaces
Plantation	Areas with crops, olive trees, and fig trees
Natural forest	Areas dominated by trees include a mix of umbrella trees and oleander plants, as well as other types of vegetation such as shrubs, ferns, and mosses.
Water	Water bodies

3.2. The spectral indices

In this study, we utilized four vegetation indices (normalized difference vegetation index (NDVI), normalized difference greenness index (NDGI), radar vegetation index (RVI), leaf area index (LAI)) that are particularly relevant to the region aspect of the study area, which contains a rich vegetation cover. In addition, we included the normalized difference built-up index (NDBI) and normalized burn ratio + (NBR+) indices to provide further insight into the land cover changes that have occurred over the time series from 2016 to 2022. We have used SNAP (https://step.esa.int/main/download/snap-download/) and ArcGis applications for the calculation of these indices. The results obtained from this analysis are presented in Figure 3 which demonstrates the extent of the changes that have taken place in the study area during this period. It is worth noting that the study area has been affected by forest fires on an annual basis since 1998, which, along with erosion, represents the most significant factors of change in the region. To better understand the changes taking place, we have also considered the impact of human activities, such as the build-up and other anthropogenic factors, on the study area. In Table 2, we define these indices. It is worth mentioning that the results obtained for Leaf Area Index (LAI) and Normalized Difference Green Index (NDGI) were found to be quite similar in this selected study area. As such, we have decided to exclusively present the NDGI results in the figure provided for the sake of conciseness and simplicity.

Table. The selected spectral indices for our study.

Index	Formula	Sentinel 2	Reference
NDVI	(NIR – RED) / (NIR + RED)	(B8 – B4) / (B8 + B4)	[17]
NDGI	(NIR-GREEN) / (NIR+GREEN)	(B8 – B3) / (B8 + B3)	[25]
RVI	(NIR) / (RED)	(B8) / (B4)	[26]
LAI	(3.618 * EVI - 0.118)	(3.618 * EVI - 0.118)	[12]
EVI	(2.5 * (NIR - RED)) / (NIR + 6 * RED - 7.5 * BLUE + 1))	(2.5 * (B8 - B4)) / (B8 + 6 * B4 - 7.5 * B2 + 1))	[13]
NDBI	(SWIR – NIR) / (SWIR + NIR)	(B11 – B8) / (B11 + B8)	[27]
NBR	(NIR-SWIR) / (NIR + SWIR)	(B8 – B12) / (B8 + B12)	[28]
NBR+	(SWIR − NIR − GEEN − BLUE) / (SWIR + NIR + GEEN + BLUE)	(B12 − B8A − B3 − B2) / (B12 + B8A + B3 + B2)	[15]

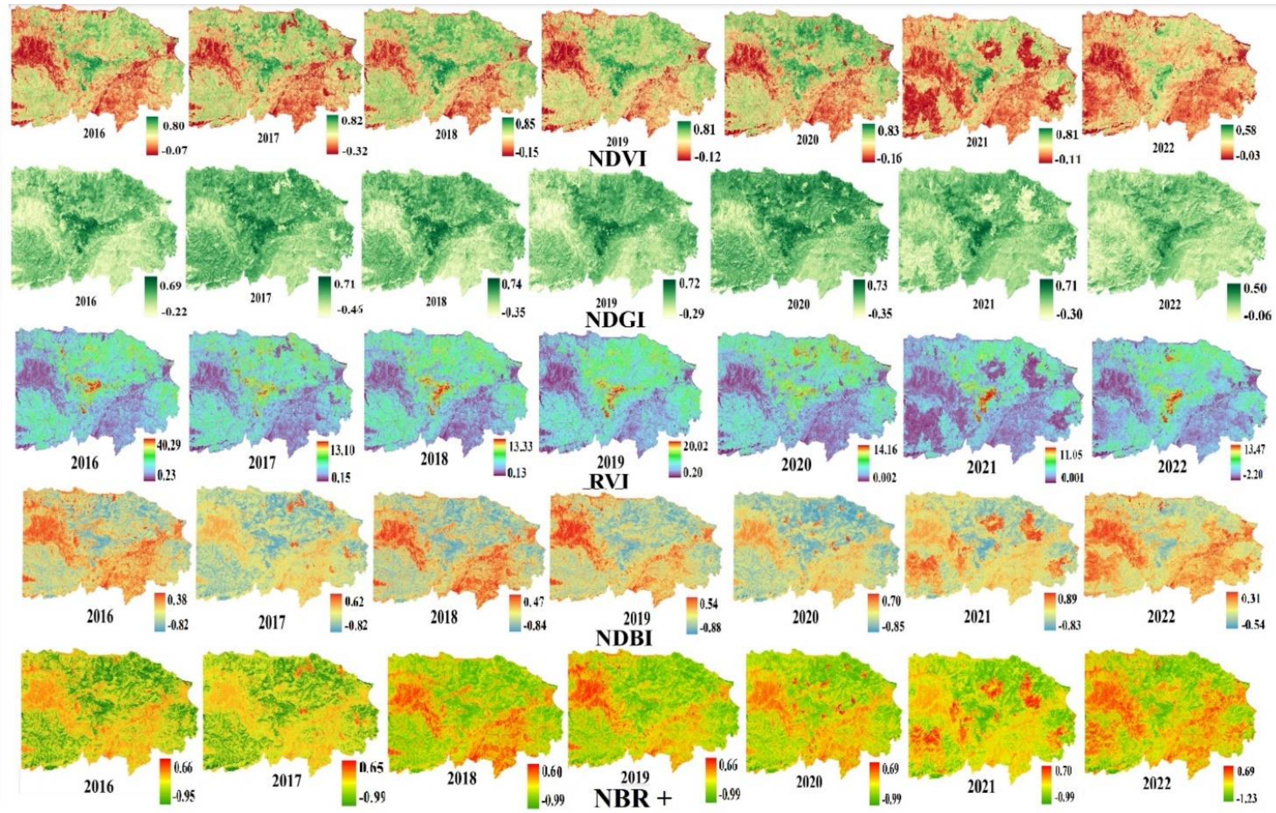

Figure 3. The selected spectral indices for the study area from 2016 to 2022.

3.3. Machine learning for LULC

With the increasing availability of satellite imagery and the advancement of machine learning algorithms, Convolutional Neural Networks (CNNs) have become a popular tool for analyzing Land Use Land Cover (LULC) changes [29, 30]. Convolutional neural networks are a type of deep learning algorithm that can automatically learn to recognize and classify objects in images. They have become increasingly popular in recent years due to their ability to achieve high accuracy in image classification tasks, even in complex scenarios. CNNs have been found to be effective in analyzing and predicting LULC changes when combined with Geographic Information Systems (GIS) technology.

For our study, we utilized ArcGIS Pro version 3.1.0 as our geographic information system software to process and analyze spatial data. Additionally, we selected the ResNet 50 convolutional neural networks (CNN) as our deep learning model of choice to perform image classification tasks. The ResNet 50 is a popular CNN architecture that has shown remarkable accuracy in object recognition tasks, and it has been widely used in various applications, including remote sensing and image processing.

4. Results

The application of CNN and change detection for LULC change analysis in our study area from 2016 to 2022 has yielded to significant results. For all our experiments, we have used a 12th Gen Intel(R) Core (TM) i9-12900H 2.50 GHz processor with 32 GB RAM. In Figure 4, we give the CNN-LULC changes. The results show that there has been a noticeable change in the bare land class for the years 2017 and 2020. This observation is consistent with the reported number of fires in the region during these years, with the regional authorities of Tizi Ouzou reporting 376 fires in 2017 and 402 fires in 2020. The 2021 data also highlighted significant forest changes in the region due to a large fire that affected the area. Interestingly, despite the high number of fires reported in the region during the summer of 2019 (485 fires in Tizi Ouzou alone), they did not appear in the classified map. It is possible that the fires were too small and scattered in different areas, making them difficult to detect using remote sensing data. The results also show that the CNN model has missed the classification for both the settlement and plantation classes. One of the main reasons for this is the overlap of these classes in reality. Settlements in the study area are surrounded by olive trees and plantation areas, making it difficult for the CNN model to accurately distinguish between them. Additionally, the plantations in the region are heavily dependent on rainfall, which makes a large portion of the plantation area a seasonal agriculture area. This dynamic nature of plantation areas can make it challenging for the CNN model to accurately classify them based on spectral information alone. These limitations are common in LULC mapping efforts that rely solely on remote sensing data. Therefore, it is important to complement remote sensing with other data sources and field observations to improve the accuracy of LULC classification in areas with complex and overlapping land cover patterns. The change detection results are given in Table 3 and are illustrated in Figure 5 (A).

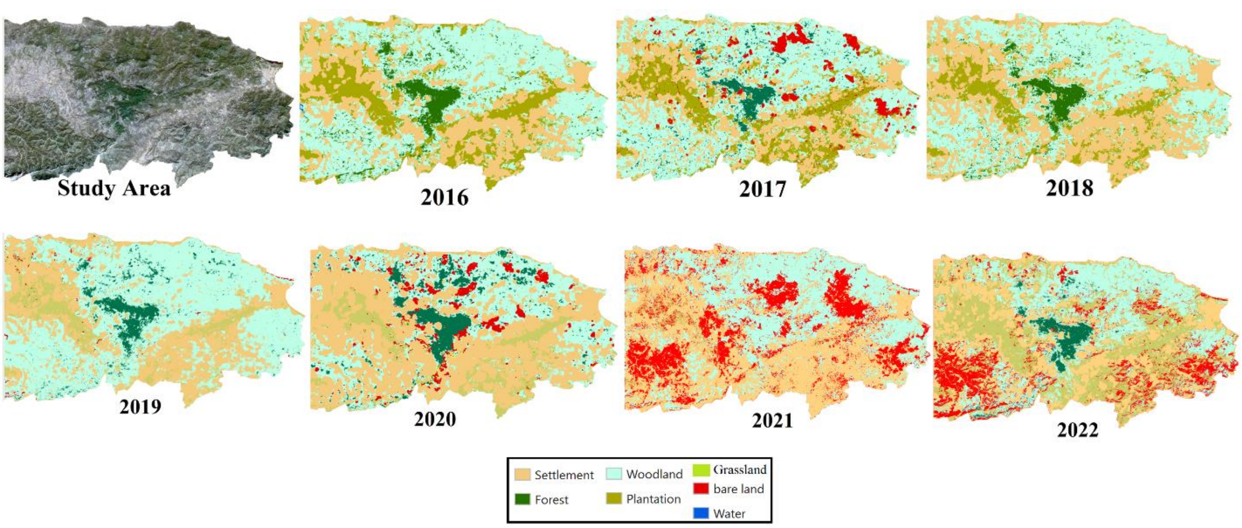

Figure 4. The CNN classification results over our study area from 2016 to 2020.

The results given by the USGS data have successfully classified the changes in the study area using more classes, capturing the shapes of most present land cover classes. However, we observed that both the settlement and plantation zones were missed and were replaced by the herbaceous class, as shown in Figure 5 (B). To verify the changes more efficiently, we decided to use a CNN-object detection process with high-resolution Planetscope images to highlight the presence of build-up areas in the selected zones. This method allowed us to overcome the limitations of both the USGS data and Sentinel 2 images classification and accurately detect the changes in the settlement areas, which are important for understanding the land use dynamics in the region.

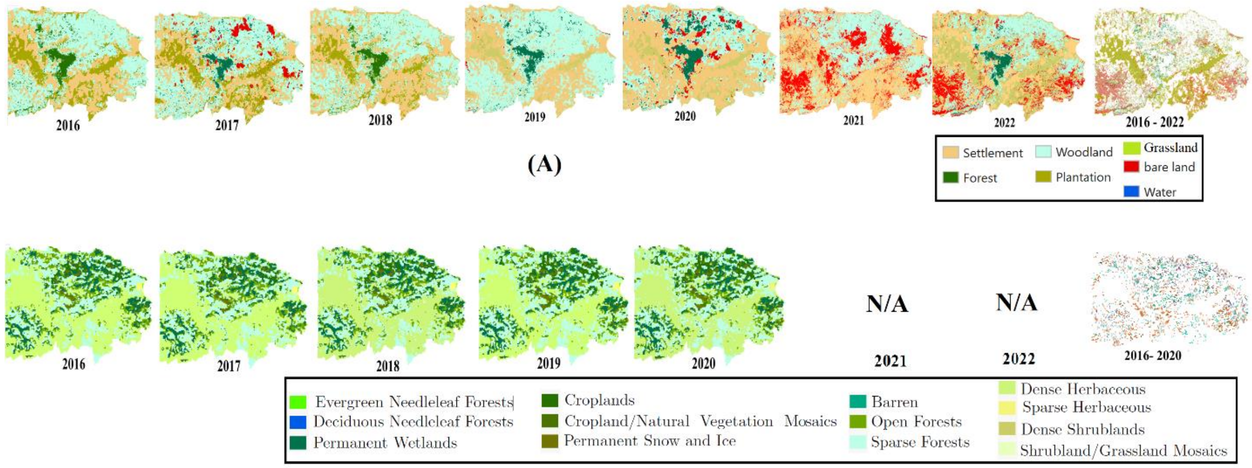

(B)

Figure 5. LULC changes over the study area. (A) Sentinel 2 images with CNN-LULC change detection from 2016 to 2022. (B) USGS data from 2016 to 2020.

In Table 3, results of area change are given for both USGS and Sentinel 2. To highlight that for the USGS data, the results for the two years 2021 and 2022 are not available. These results are also illustrated in Figure 6.

Table 3. Area change with different classes changes for Sentinel 2 images and USGS data.

Detection Change form 2016 to 2020				Detection Change form 2016 to 2022	
Sentinel 2 with CNN		USGS Land Cover Change		Sentinel 2 with CNN	
Class_name	Area (ha)	Class_name	Area (ha)	Class_name	Area (ha)
Settlement->Forest	110	Evergreen Needleleaf Trees->Sparse Herbaceous	21	Settlement->Forest	5
Settlement->Woodland	2,138	Permanent Wetlands->Croplands	2,640	Settlement->Woodland	3,507
Settlement->Plantation	2,610	Permanent Wetlands->Cropland/Natural Vegetation	86	Settlement->GrassLand	1
Settlement->Greenland	67	Permanent Wetlands->Non-Vegetated Lands	1,760	Settlement->Plantation	26,814
Settlement->land bare	229	Permanent Wetlands->Open Forests	1,996	Settlement->land bare	8,403
Forest->Settlement	2,667	Permanent Wetlands->Sparse Forests	1,009	Forest->Settlement	1,329
Forest->Woodland	3,706	Permanent Wetlands->Dense Herbaceous	86	Forest->Woodland	6,009
Forest->Plantation	265	Croplands->Permanent Wetlands	236	Forest->GrassLand	58
Forest->Greenland	307	Croplands->Cropland/Natural Vegetation	43	Forest->Plantation	4,149
Forest->land bare	1,846	Croplands->Non-Vegetated Lands	86	Forest->land bare	1,039
Woodland->Settlement	48,561	Croplands->Open Forests	322	Woodland->Settlement	10,136
Woodland->Forest	12,150	Croplands->Sparse Forests	558	Woodland->Forest	3,627
Woodland->Plantation	3,988	Croplands->Dense Herbaceous	43	Woodland->GrassLand	7
Woodland->Greenland	251	Cropland/Natural Vegetation->Non-Vegetated Lands	64	Woodland->Plantation	32,430
Woodland->land bare	13,659	Non-Vegetated Lands->Permanent Wetlands	21	Woodland->land bare	34,443
Plantation->Settlement	24,998	Non-Vegetated Lands->Croplands	580	Plantation->Settlement	5,428
Plantation->Forest	742	Non-Vegetated Lands->Open Forests	64	Plantation->Forest	7
Plantation->Woodland	6,080	Mixed Broadleaf Evergreen->Cropland/Natural Vegetation	43	Plantation->Woodland	3,618
Plantation->Greenland	1,079	Mixed Broadleaf Evergreen->Open Forests	21	Plantation->Plantation	49,048
Plantation->land bare	1,814	Open Forests->Permanent Wetlands	4,894	Plantation->land bare	5,015
bare land->Settlement	0	Open Forests->Croplands	644	bare land->Settlement	0
bare land->Woodland	1	Open Forests->Cropland/Natural Vegetation	258	bare land->Woodland	1
bare land->Plantation	0	Open Forests->Non-Vegetated Lands	708	bare land->Plantation	0
Water->Settlement	29	Open Forests->Sparse Forests	7,878	bare land->land bare	0
Water->Forest	0	Open Forests->Dense Herbaceous	1,889	Water->Settlement	1
Water->Woodland	88	Sparse Forests->Permanent Wetlands	1,202	Water->Forest	0
Water->Plantation	47	Sparse Forests->Croplands	2,147	Water->Woodland	1
Water->land bare	1	Sparse Forests->Cropland/Natural Vegetation	301	Water->Plantation	56
No Change	244,403	Sparse Forests->Non-Vegetated Lands	86	No Change	176,705
		Sparse Forests->Mixed Broadleaf Evergreen	64		
		Sparse Forests->Open Forest	5,581		
		Sparse Forests->Dense Herbaceous	6,139		
		Sparse Forests->Sparse Herbaceous	43		
		Dense Herbaceous->Permanent Wetlands	429		
		Dense Herbaceous->Croplands	129		
		Dense Herbaceous->Non-Vegetated Lands	107		
		Dense Herbaceous->Open Forest	3,799		
		Dense Herbaceous->Sparse Forest	17,924		
		Dense Herbaceous->Sparse Herbaceous	215		
		Dense Herbaceous->Sparse Shrublands	43		
		Sparse Herbaceous->Sparse Forest	129		
		Sparse Herbaceous->Dense Herbaceous	43		
		Dense Shrublands->Open Forest	21		
		Dense Shrublands->Sparse Forest	21		
		Dense Shrublands->Dense Herbaceous	86		
		Shrubland/Grassland Mosaics->Sparse Forest	21		
		No Change	307,347		

In order to identify the Settlement class that was previously missed by the USGS data and not accurately highlighted by Sentinel 2 results, a convolutional neural network (CNN) object detection approach was utilized. Specifically, the RCNN mask was selected as the most appropriate technique for this task. In order to compare the results obtained from the three different data sources, Sentinel 2, USGS data, and Planetscope, the most recent available image for USGS is the 2020 image. Thus, the comparison was performed using the 2020 images from each of the sources.

By using this method, the CNN was able to accurately detect and label the areas where Settlement class was present, allowing for a more comprehensive and precise analysis of the geographical area in question. This approach has proven to be highly effective in detecting the two classes. Results are shown in Figure 6.

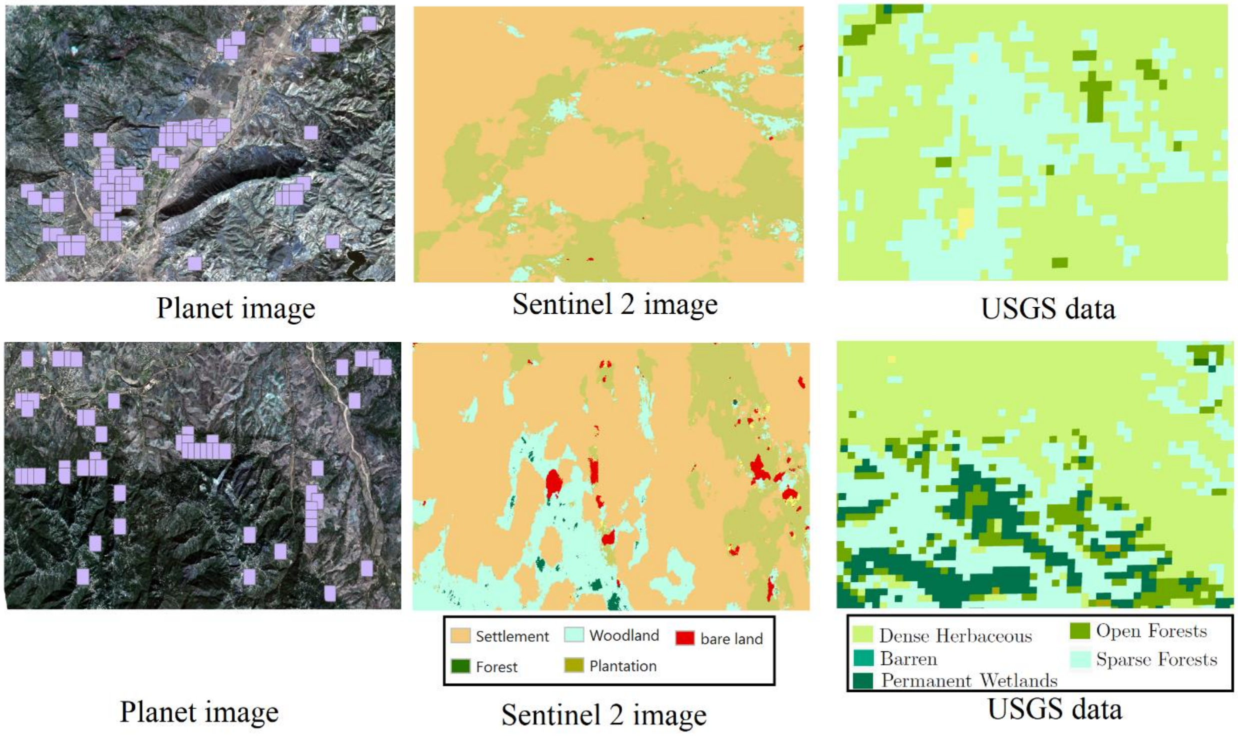

Figure 6. Comparison between the Settlement class detection for the three used sources (Planet image, Sentinel 2 image, and USGS data).

Conclusion

This study aimed to classify land use and land change in a selected area of North Algeria, utilizing a combination of spectral indices and a convolutional neural network (CNN) land use land change (LULC) change detection approach with Sentinel 2 images. The results obtained by the approach were promising. However, certain classes were not adequately detected by the Sentinel 2 images, which required the use of object detection with Planetscope images to efficiently highlight their presence. Despite the high spatial resolution of Planetscope images and the high spectral resolution (with 13 bands) of Sentinel 2 images, it is crucial to complement remote sensing with other data sources and field observations for accurate classification and change detection. This approach can provide a more comprehensive and accurate understanding of land use and land change dynamics in the study area.

References

[1] Mahdavi, S., Salehi, B., Huang, W., Amani, M., Brisco, B., "A PolSAR Change Detection Index Based on Neighborhood Information for Flood Mapping," Remote Sens., 11, 1854, (2019).

[2] Seydi, S.T., Hasanlou, M., Amani, M. A, "New end-to-end multi-dimensional CNN framework for land cover/land use change detection in multi-source remote sensing datasets," Remote Sensing 2020, 12, 2010.

[3] Hasanlou, M., Seydi, S.T., Shah-Hosseini, R. A., "Sub-Pixel Multiple Change Detection Approach for Hyperspectral Imagery," Can. J. Remote Sens., 44, 601–615, (2018).

[4] Wang, M., Tan, K., Jia, X., Wang, X., Chen, Y., "A Deep Siamese Network with Hybrid Convolutional Feature Extraction Module for Change Detection Based on Multi-sensor Remote Sensing Images," Remote Sens., 12, 205, (2020).

[5] da Silva, V. S., Salami, G., da Silva, M. I. O., Silva, E. A., Monteiro Junior, J. J., & Alba, E., "Methodological evaluation of vegetation indexes in land use and land cover (LULC) classification," Geology, Ecology, and Landscapes, 4(2), 159-169, (2020).

[6] Zhang, Y.; Kerle, N., "Satellite remote sensing for near-real time data collection," In Geospatial Information Technology for Emergency Response; CRC Press: Boca Raton, FL, USA, pp. 91–118, (2008).

[7] Tian, T., Zhu, Y.L., Hu, F.H., Wang, Y.Y., Huang, N.P., Xiao, Z.D., "Dynamics of exosome internalization and trafficking," J. Cell. Physiol., 228, 1487–1495, (2013).

[8] Xu, C., Ding, Y., Zheng, X., Wang, Y., Zhang, R., Zhang, H., ... & Xie, Q., "A Comprehensive Comparison of Machine Learning and Feature Selection Methods for Maize Biomass Estimation Using Sentinel-1 SAR, Sentinel-2 Vegetation Indices, and Biophysical Variables," Remote Sensing. 14, 4083, (2022).

[9] Pettorelli, N., Vik, J.O., Mysterud, A., Gaillard, J.M., Tucker, C.J., Stenseth, N.C. Using the satellite-derived NDVI to assess ecological responses to environmental change. Trends Ecol. Evol. 2005, 20, 503–510.

[10] Huang, S., Tang, L., Hupy, J. P., Wang, Y., & Shao, G., "A commentary review on the use of normalized difference vegetation index (NDVI) in the era of popular remote sensing," Journal of Forestry Research, 32(1), 1-6, (2021).

[11] Gilabert, M. A., González-Piqueras, J., Garcıa-Haro, F. J., & Meliá, J., "A generalized soil-adjusted vegetation index," Remote Sensing of environment, 82(2-3), 303-310, (2002).

[12] Fang, H., Baret, F., Plummer, S., & Schaepman-Strub, G., "An overview of global leaf area index (LAI): Methods, products, validation, and applications," Reviews of Geophysics, 57(3), 739-799, (2019).

[13] Xie, F., & Fan, H., "Deriving drought indices from MODIS vegetation indices (NDVI/EVI) and Land Surface Temperature (LST): Is data reconstruction necessary?," International Journal of applied earth observation and geoinformation, 101, 102352, (2021).

[14] Watson, C. S., King, O., Miles, E. S., & Quincey, D. J., "Optimising NDWI supraglacial pond classification on Himalayan debris-covered glaciers," Remote sensing of environment, 217, 414-425, (2018).

[15] Alcaras, E., Costantino, D., Guastaferro, F., Parente, C., & Pepe, M., "Normalized Burn Ratio Plus (NBR+): a new index for sentinel-2 imagery," Remote Sensing, 14(7), 1727, (2022).

[16] Feng, Y., Liu, Y., & Batty, M., "Modeling urban growth with GIS based cellular automata and least squares SVM rules: a case study in Qingpu–Songjiang area of Shanghai," China. Stochastic environmental research and risk assessment, 30, 1387-1400, (2016).

[17] Chen, W., Chai, H., Zhao, Z., Wang, Q., & Hong, H., "Landslide susceptibility mapping based on GIS and support vector machine models for the Qianyang County," China. Environmental Earth Sciences, 75, 1-13, (2016).

[18] Lee, S., Hong, S. M., & Jung, H. S., "GIS-based groundwater potential mapping using artificial neural network and support vector machine models: the case of Boryeong city in Korea," Geocarto international, 33(8), 847-861, (2018).

[19] Zabihi, M., Pourghasemi, H. R., Pourtaghi, Z. S., & Behzadfar, M., “GIS-based multivariate adaptive regression spline and random forest models for groundwater potential mapping in Iran,” Environmental Earth Sciences, 75, 1-19, (2016).

[20] Alshari, E. A., & Gawali, B. W., “Development of classification system for LULC using remote sensing and GIS,” Global transitions proceedings, 2(1), 8-17, (2020).

[21] Dewangkoro, H. I., & Arymurthy, A. M., “Land use and land cover classification using CNN, SVM, and channel squeeze & spatial excitation block,” In IOP Conference Series: Earth and Environmental Science (Vol. 704, No. 1, p. 012048). IOP Publishing, (2021, March).

[22] Lv, Q., Dou, Y., Niu, X., Xu, J., Xu, J., & Xia, F., “Urban land use and land cover classification using remotely sensed SAR data through deep belief networks,” Journal of Sensors, (2015)..

[23] Azad, A., & Wang, X., “Land use change ontology and traffic prediction through recurrent neural networks: A case study in Calgary, Canada,” ISPRS International Journal of Geo-Information, (2021).

[24] Salhi, C., Touaibia, B., Zeroual, A., Benblida, N., & Assani, A., “Evaluation of soil erosion in Northern Algeria watershed using SWAT and RUSLE models,” *Geocarto International*, 1-31, (2022).

[25] Nedkov, R, “Normalized Differential Greenness Index for vegetation dynamics assessment,” Comptes rendus de l’Academie bulgare des Sciences, 70(8), 1143-1146, (2017).

[26] Cohen, W., “Response of vegetation indices to changes in three measures of leaf water stress. Photogramm,” Eng. Remote Sens. 57(2), 195–202, (1991).

[27] Kuc, G., & Chormański, J., “Sentinel-2 imagery for mapping and monitoring imperviousness in urban areas,” The International Archives of the Photogrammetry, Remote Sensing and Spatial Information Sciences, 42, 43-47, (2019).

[28] Filipponi, F., “BAIS2: Burned area index for Sentinel-2,” In Proceedings (Vol. 2, No. 7, p. 364), MDPI, (2018, March).

[29] Tegegne, A. M., “Applications of convolutional neural network for classification of land cover and groundwater potentiality zones,” Journal of Engineering, 1-8, (2022).

[30] Zhang, C., Sargent, I., Pan, X., Li, H., Gardiner, A., Hare, J., & Atkinson, P. M., “Joint Deep Learning for land cover and land use classification,” Remote sensing of environment, 221, 173-187, (2019).